Expanded View Figures

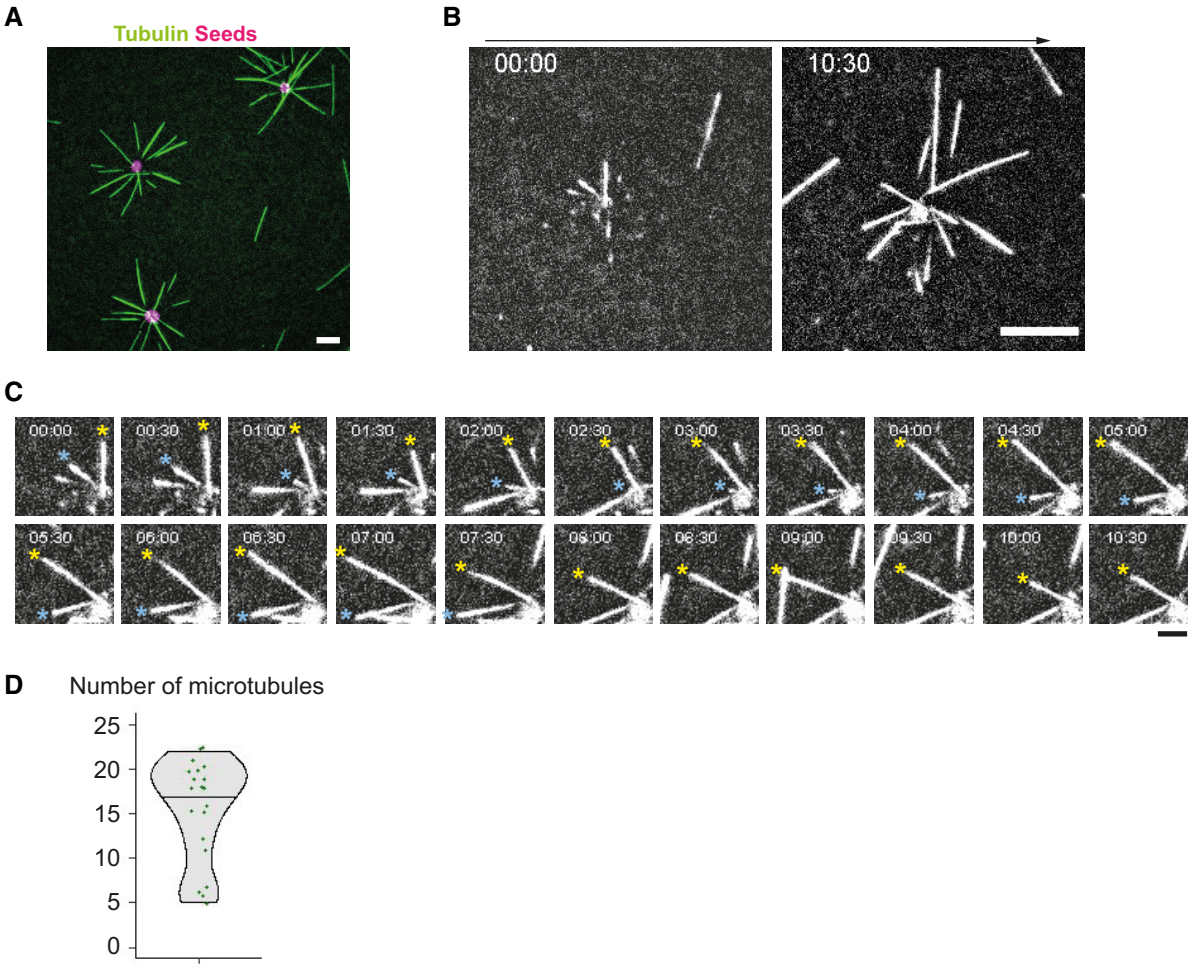

Figure EV1. Characterization of an artificial MTOC.

A Observation of MT aster formation using TIRF microscope. Scale bar = 10 μm.
B Time-lapse imaging of the MT aster formation using TIRF. Scale bar = 10 μm.
C Magnified images of (B). Time interval 30 s. Time bar indicates (min:sec). MTs showing dynamic instability were indicated with asterisks. Scale bar = 5 μm.
D Number of MTs emanating from the aMTOCs in microwells. Tubulin 18 μM. *n* = 20 wells. Violin plots were shown with the median (horizontal line).

Figure EV2. Characterization of aMTOC positioning in microwells.

A Consideration of the probability of aMTOC distribution. When the volumes of six segments (equal intervals from well center) are considered as shown in the left scheme, the volume per segment increases from well center toward well edge (left histogram), suggesting that the probability of the aMTOC distribution increases from well center toward the edge. Middle histogram shows experimental probability of the aMTOC position in the absence of free tubulin and actin (*n* = 188 wells). The probability tended to increase from well center toward the edge. However, the distribution near the edge was restricted, because of the size of aMTOCs (bead 1.5 μm radius + MT seeds). Right histogram indicates probability per volume, suggesting almost random distribution of the aMTOCs in microwells. Volume per segment was calculated based on the approximate size of microwells (37.5 μm in diameter and 20 μm in height).
B Distribution of aMTOC in microwells at the indicated tubulin concentrations. Probability per volume was calculated as shown in (A). Data shown in Fig 1G were used.
C Time-lapse imaging of MT aster positioning at 18 μM of tubulin shown in Fig 1H. In magnified images, the orange dots indicate the MTs hitting the well edge.
D Time-lapse imaging of MT aster positioning at 26 μM of tubulin shown in Fig 1J. In magnified images, the blue and yellow arrow heads indicate the MTs slipping along the well edge, respectively.

Data information: Scale bar = 10 μm.

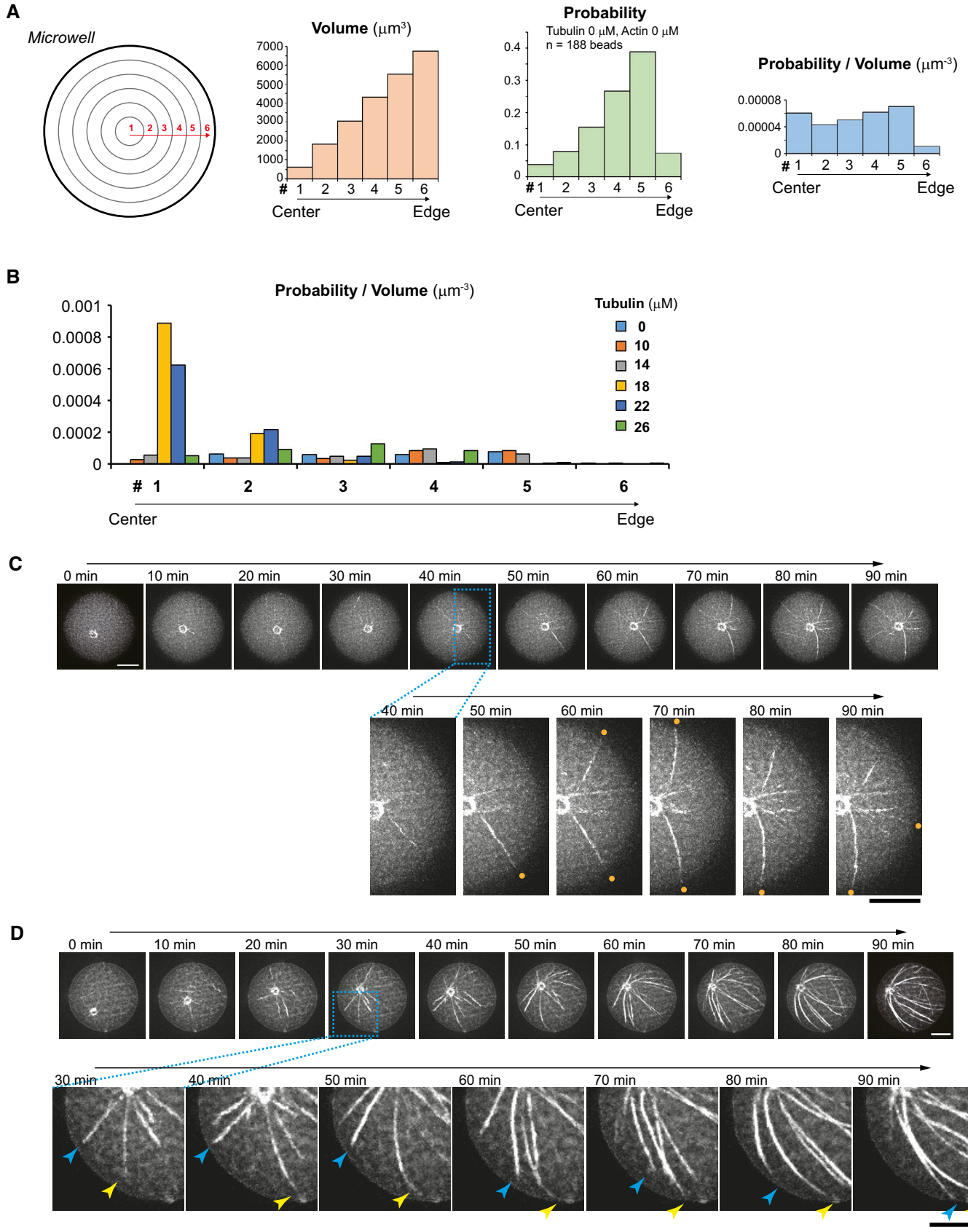

Figure EV2.

Figure EV3. aMTOC positioning in the presence of bulk actin network.

A Distribution of aMTOC in microwells in the presence of the indicated tubulin and actin concentrations. Probability per volume was calculated as shown in Fig EV2A. Data shown in Fig 3B were used.

B The path length (cumulative distance) of the aMTOC during the time-lapse imaging was measured for the indicated conditions. The data of individual aMTOC were shown with different colors (10 aMTOCs per condition). Images were taken at 1-min intervals.

C Distribution of the aMTOC in microwells in the presence of tubulin 26 μM and bulk actin 4 μM. Probability per volume was calculated as shown in Fig EV2A. Data from Fig 3B. Scale bar = 50 μm.

D Simulation in the presence of bulk actin network. Even with longer MT formation (compared with Fig 3E), the MTOC centering was not occurred. Different time points (75 and 250 s) were shown. Right graph shows trajectories from blue (0 s) to red (250 s). MTOC—gray, MT—black, actin—pink.

E Simulations in the presence of lower density of actin. Different time points (25, 50, 100, and 150 s) were shown. Middle graph shows trajectories from blue (0 s) to red (150 s). Right graph shows the final position of MTOC (at 150 s). Data of the absence of actin (left) are same as shown in Fig 3G. ns (not significant) > 0.1 (Mann–Whitney *U* test). Fifteen simulations per condition.

F Simulations in the presence of smaller number of MTs. The images represent the time point at 150 s. Right graph shows the final position of MTOC (at 150 s). ****$P < 0.0001$ (Mann–Whitney *U* test). Fifteen simulations per condition.

Data information: Violin plots were shown with the median (horizontal line).

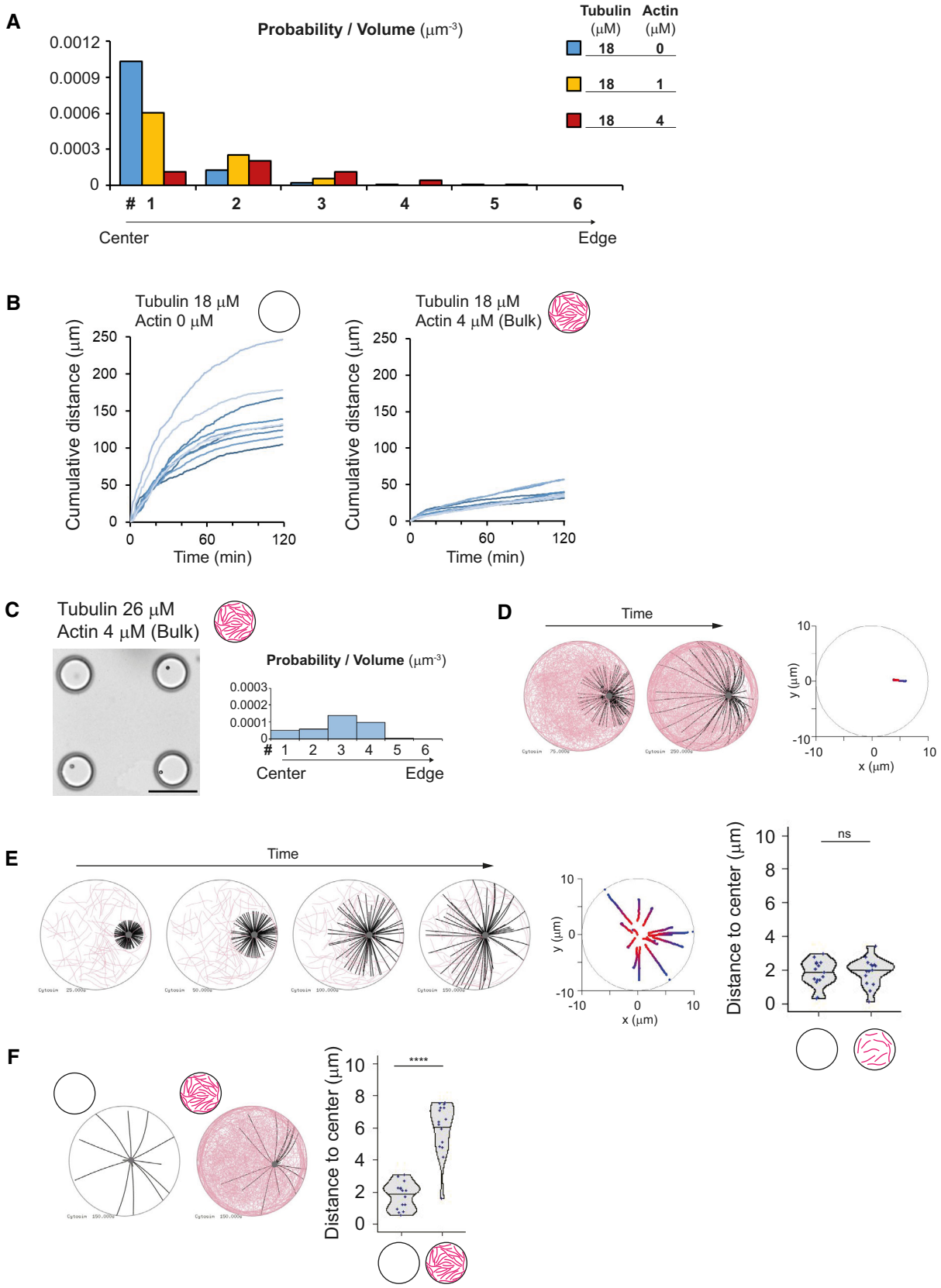

Figure EV3.

Figure EV4. Characterization of aMTOC positioning and MT behaviors in the absence or presence of cortical actin network.

A Distribution of the aMTOC in microwells in the presence of the indicated tubulin and actin concentrations. Probability per volume was calculated as shown in Fig EV2A. Data shown in Fig 4B were used.

B Time-lapse imaging of MT aster positioning at 26 μM of tubulin in the presence of cortical actin shown in Fig 4F. Magnified images were shown. Scale bar = 10 μm.

C Orientation of MTs around the MTOCs in the absence or presence of cortical actin. The samples were same as shown in Fig 4E and F. Orientation of MTs was shown with different colors. Scale bar = 10 μm.

D Other representatives showing orientation of MTs near the well edge in the absence or presence of cortical actin. Orientation of MTs was shown with different colors. Right graph indicates the measurement of the MT orientation using Orientation J. The different time points were shown with different colors. Scale bar = 10 μm.

E The path length (cumulative distance) of the aMTOC during the time-lapse imaging was measured for the indicated conditions. The data of individual aMTOC were shown with different colors (10 aMTOCs per condition). Images were taken at 10-min intervals.

F Simulations of MTOC position over time in the absence (left) or presence (right) of cortical actin. Fifteen simulations per condition were shown with different colors.

G Simulations in the presence of smaller number of MTs. The images represent the time point at 200 s. Right graph shows the final position of MTOC (at 200 s). ****$P < 0.0001$ (Mann–Whitney U test). Fifteen simulations per condition.

H Distribution of the aMTOC in microwells in the presence of tubulin 18 μM and cortical actin 2 μM. Probability per volume was calculated as shown in Fig EV2A. Data shown in Fig 4B were used. Scale bar = 50 μm.

I aMTOC position in the presence of 26 μM tubulin and with less dense cortical actin assembled at a lower concentration of actin (0.5 μM). Right panel shows measurement of distance from aMTOC to center of the well (2 h after sample preparation). $n = 71$ wells. Scale bar = 50 μm.

J Simulations in the presence of lower density of cortical actin. The time points at 200 s were shown. Right graph shows the final position of MTOC (at 200 s). Data of the absence of actin (left) are same as shown in Fig 4M. ns (not significant) > 0.1 (Mann–Whitney U test). Fifteen simulations per condition.

Data information: Violin plots were shown with the median (horizontal line).

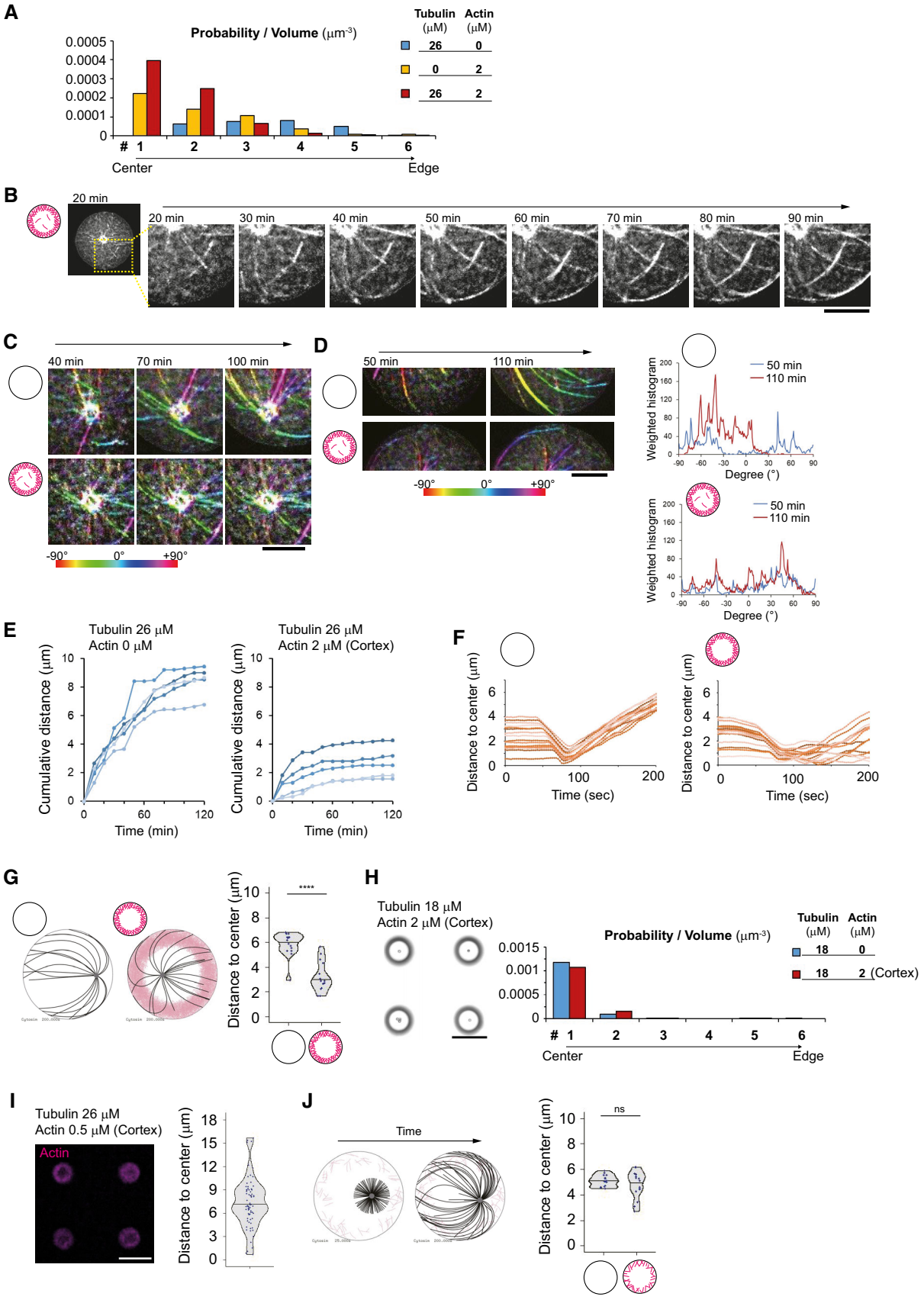

Figure EV4.

Figure EV5. aMTOC positioning in the presence of asymmetric actin network.

A Detection of actin inner zone. Actin 0.5 μM and a-actinin 100 nM with Arp2/3 complex and NPF (WA) coating. The bottom and top were excluded from the maximum projection to visualize the vertical edges of actin. Using the partial max projection images and defining a threshold of actin intensity, the region of actin inner zone was detected and the center (centroid) was measured. Scale bar = 50 μm.

B Measurement of the fluorescence intensity of actin. The red arrow in the image indicates the region used for the line scan analysis. Right graph indicates the result of the line scan analysis. Background signals outside the wells were subtracted. The less actin region inside the cortex was defined as the actin inner zone. Scale bar = 10 μm.

C, D To analyze the aMTOC position with respect to the asymmetry of cortical actin, the angles from the well center to the center of the actin inner zone were aligned at the same degree (0°). It means that wells were reoriented in order to align the angles from the well center to the center of the actin inner zone.

E Distance from aMTOC to well center (2 h after sample preparation). Data shown in Fig 5E and F, and I were used. (Tubulin 26 μM Actin 0 μM, $n = 65$, Tubulin 0 μM Actin 0.5 μM, $n = 74$, Tubulin 26 μM Actin 0.5 μM, $n = 79$ wells) ***$P < 0.001$, ****$P < 0.0001$, ns (not significant) > 0.1 (Kruskal–Wallis test with Dunn's multiple comparison test). Violin plots were shown with the median (horizontal line).

F, G Distribution of the aMTOC in microwells in the presence of tubulin and actin at the indicated concentrations. Probability per volume was calculated as shown in Fig EV2A. Data shown in Figs EV5E and 5J were used for (F) and (G), respectively.

H Simulations in the presence of asymmetric actin when the initial position was randomly chosen within 4 μm from cell center. Twenty-five simulations per condition. Different time points (From left, 25, 100, and 250 s) were shown. Even if the initial position is off-centered, the MTOC tended to migrate toward the thinner side of the actin network. ***$P < 0.001$ (Mann–Whitney U test). Violin plots were shown with the median (vertical line).

I Simulations in the presence of smaller number of MTs. The images represent the time point at 250 s. Lower graph shows the final position of MTOC (at 250 s). Twenty-five simulations per condition. Violin plots were shown with the median (vertical line).

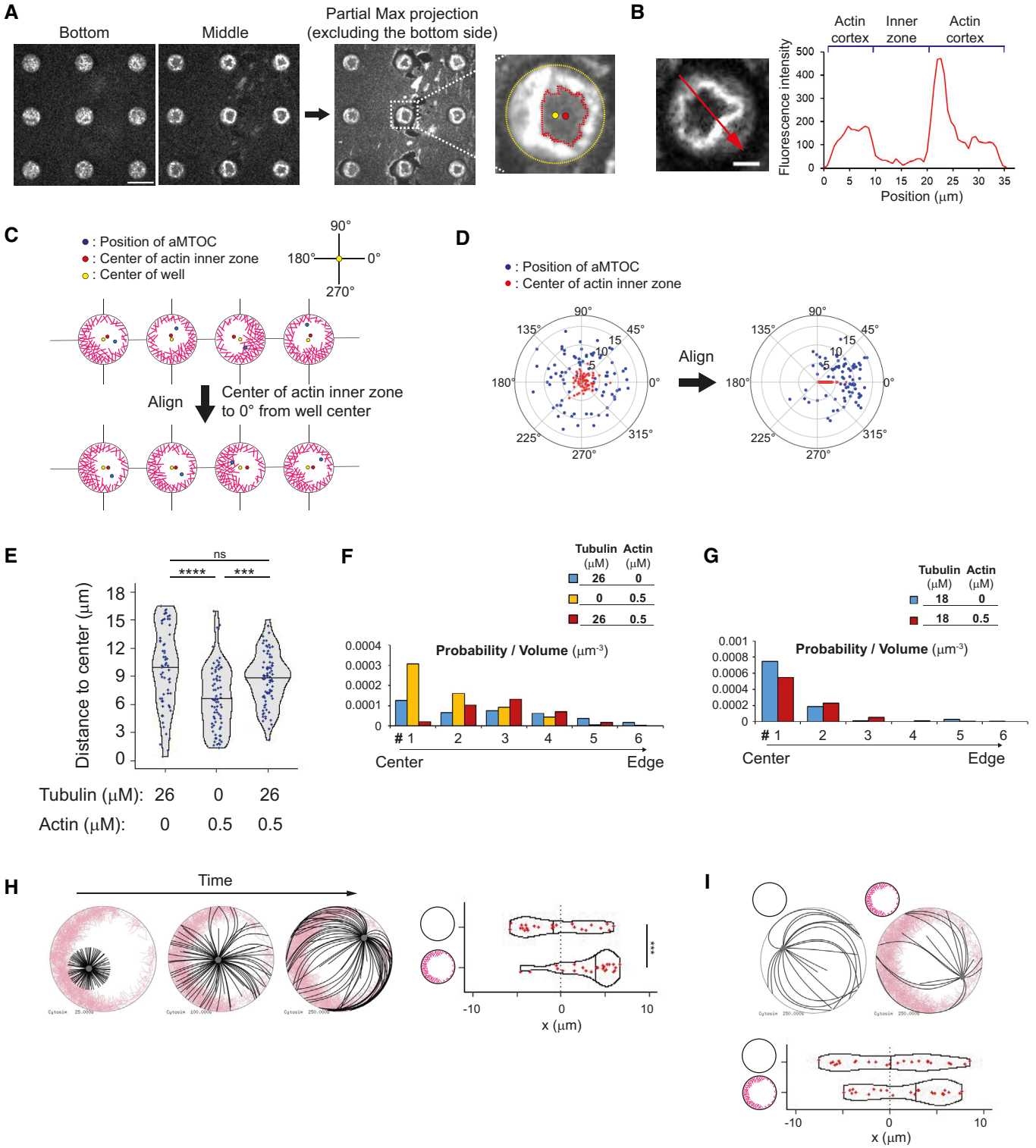

Figure EV5.